SAND2014-15517D

Development of Mechanically and Environmentally Stable Oxide Coatings using Pulsed Laser Irradiation

PURDUE ENGINEERING MATERIALS ENGINEERING

S.K. Lawrence[1], D.P. Adams[2], D.F. Bahr[1], N.R. Moody[2]

1. Purdue University ; 2. Sandia National Laboratories

Sandia National Laboratories

Objective & Characterization Methods

Nanosecond pulsed laser irradiation of ***stainless steel 304L*** and ***CP Grade II titanium*** substrates leads to the growth of highly colored oxide films for use as passive indicators of tamper in welded or sealed components of energy systems. Oxide morphology and phase determine mechanical properties and fracture behavior. Electromechanical performance, investigated with nanoECR, and environmental resistance, evaluated with immersion and salt spray testing, were then linked to the oxide structure and laser processing conditions.

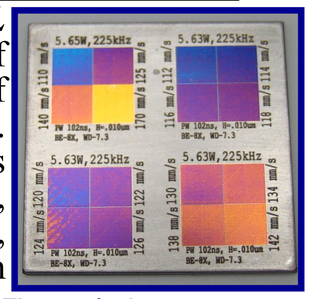

Figure 1: Colored oxides.

Oxide Structure

Microscopy, spectroscopy, and diffraction reveal formation of multiple oxides with composition gradients and highlight distinct morphology and microstructure.

Figure 2: SEM image (left) highlighting pervasive mudflat cracking on *Ti oxides*. TEM image (right) shows mixed oxide on *Ti* substrate, consisting of a Ti_6O interfacial layer and a TiO overlayer. X-ray diffraction determined oxide composition.

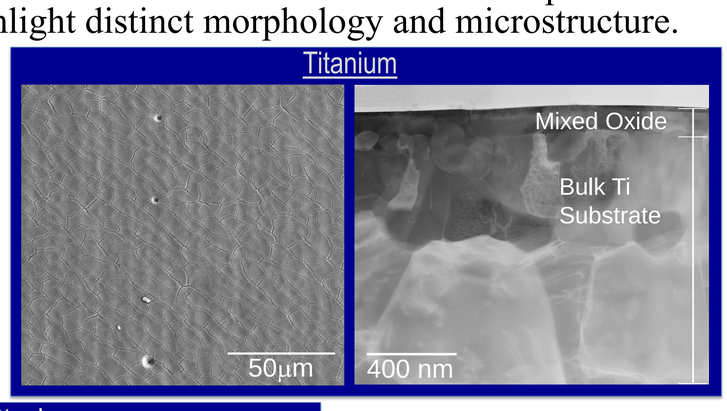

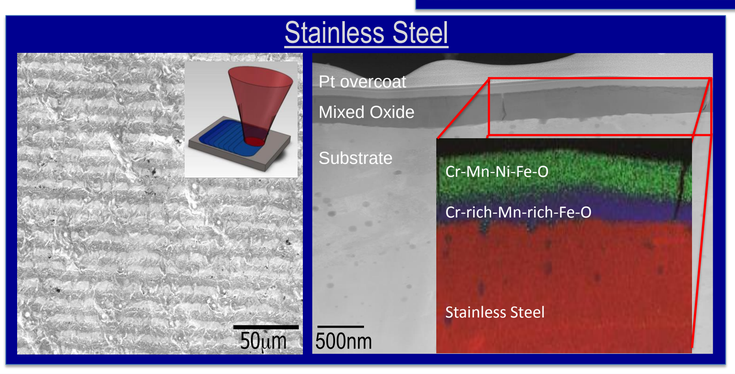

Figure 3: SEM image of *SS 304L* oxide surface showing rippled morphology (left). STEM EDS (right) reveals a sharp interface between substrate and oxide, but two distinct phases in the oxide with a composition gradient between the Cr-rich interfacial layer and the Fe-rich overlayer.

Oxide Fracture & Mechanical Behavior

Continuous stiffness measurement (CSM) yields modulus, hardness, and stiffness values. Quasi-static (QS), high-load conical indentation was used to determine load/depth at discrete oxide fracture events.

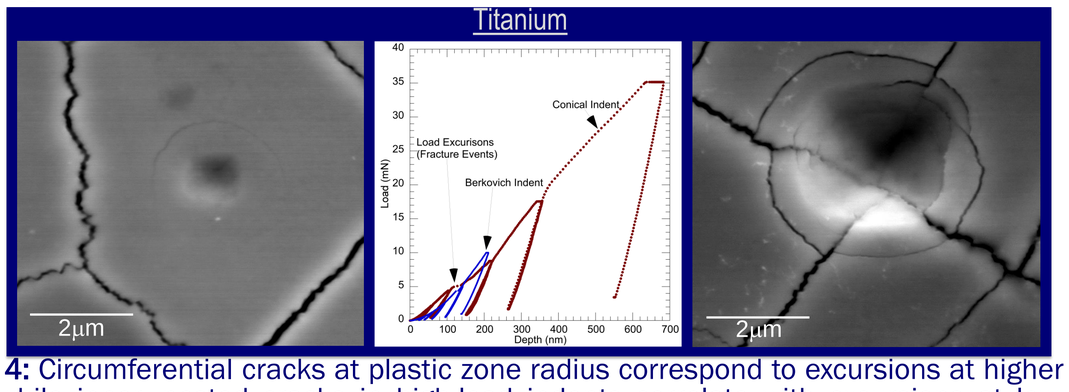

Figure 4: Circumferential cracks at plastic zone radius correspond to excursions at higher loads (left), while inner, nested cracks in high-load indents correlate with excursions at low loads (right). Examples of pop-ins in conical indents and Berkovich indents are shown (middle).

Scan Rate (mm/s)	*Thickness (nm)*	*Modulus (GPa)*	*Hardness (GPa)*	*Fracture Toughness (MPavm)*	*Residual Stress (GPa)*
130	153	217±12	16.4±0.50	3.57	5.20±1.0
140	140	215±25	15.4±0.95	2.77	3.97±0.7
150	135	214±10	15.1±2.2	2.58	3.27±0.1
160	125	213±9	19.0±1.9	2.49	3.19±0.9

Table 1: Average modulus and hardness, as well as fracture toughness and residual stress calculated from LEFM for oxides on Ti.

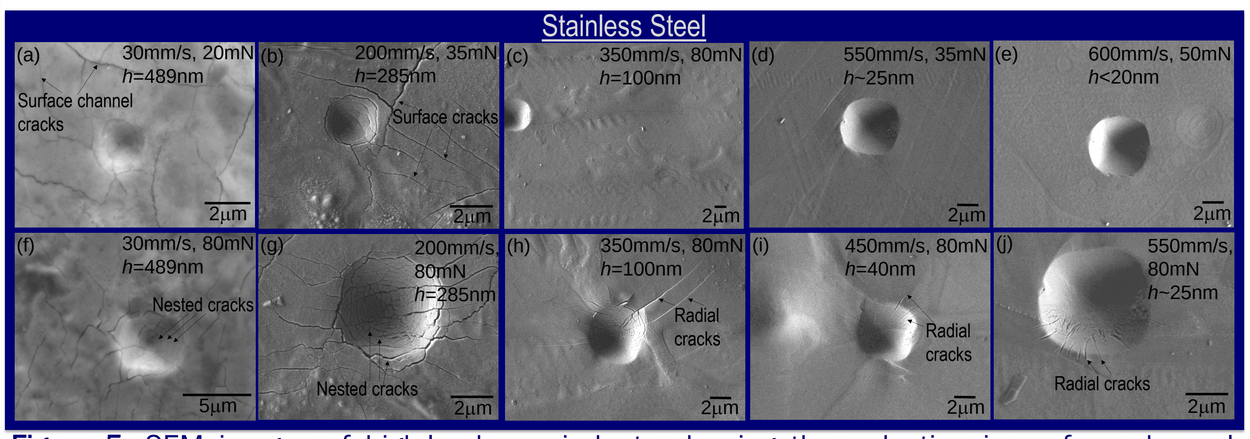

Figure 5: SEM images of high-load nanoindents showing the reduction in surface channel cracking with decreasing film thickness, *h*, (a)-(e) (increasing laser scan rate) as well as the shift from circumferential cracking to radial cracking as thickness decreases (f)-(j).

Scan Rate (mm/s)	*Thickness (nm)*	*Hardness (GPa)*	*Modulus (GPa)*	*H/E*
30	489	9.2±1.0	155±7	0.059
47	405	10.7±1.9	155±9	0.069
80	403	9.8±1.3	159±9	0.062
175	302	10.4±1.1	157±5	0.066
200	285	9.9±1.2	157±9	0.063
225	196	10.3±0.9	157±7	0.066
250	150	10.8±1.8	155±10	0.069
300	147	7.3±0.9	146±15	0.050
350	100	8.3±2.0	159±16	0.052
400	84	6.3±1.2	150±17	0.042
450	65	4.9±0.6	141±12	0.035
500	40	4.7±1.4	148±18	0.022
*550	~25	3.3±1.3	147±10	0.022
#600	<20	N/A	N/A	N/A

Table 2: Hardness, modulus, and H/E ratio of oxides tabulated as a function of laser scan rate and average oxide thickness. Values reported for contact radius to film thickness (a_c/h) ratios between 0.5 and 1.0.

Oxide Electromechanical Performance

Conducting indentation (nanoECR) indicates a correlation between laser exposure, current-voltage behavior at constant load, and indentation response.

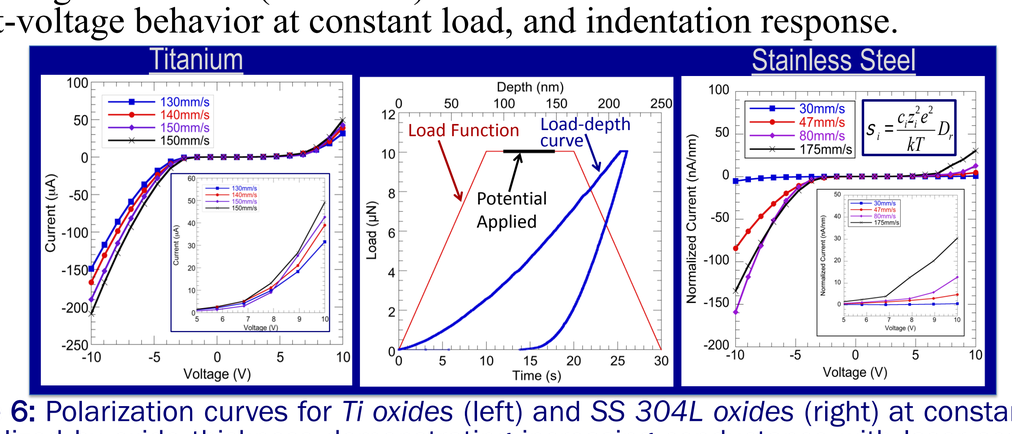

Figure 6: Polarization curves for *Ti oxides* (left) and *SS 304L oxides* (right) at constant load, normalized by oxide thickness demonstrating increasing conductance with laser scan rate. Insets on both plots show zoomed views of positive maxima. Loading regime, including segment with applied potential and resulting load-displacement curve is presented in (middle) plot. Conductance is not a function of thickness, thus the dependence on scan rate must be linked to defect density.

Oxide System Environmental Resistance

Quad-oxide ***SS 304L*** samples were immersion tested in simulated sea water for 25 days, while single oxide samples were subjected to salt spray testing for 168 hours.

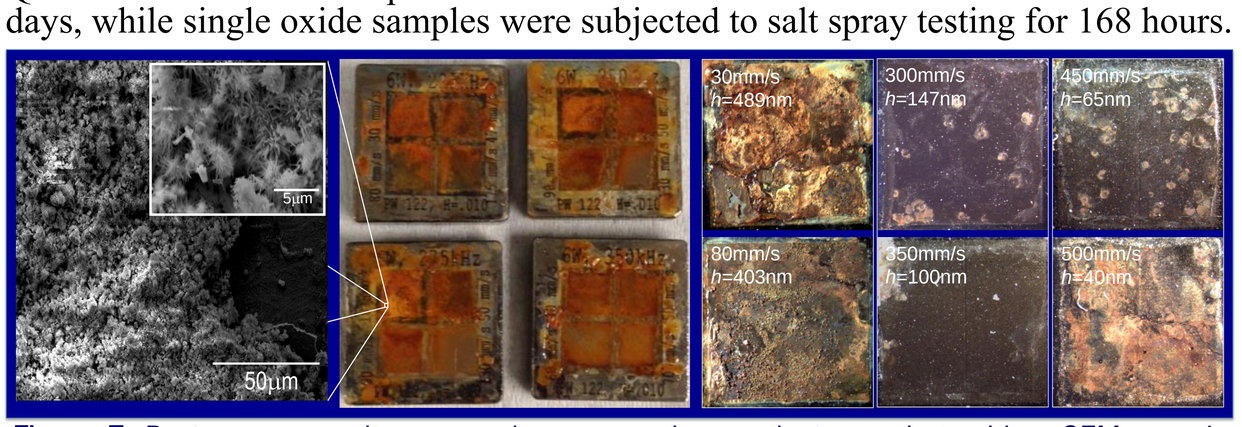

Figure 7: Post-exposure microscopy shows corrosion product covering oxides. SEM reveals product structure (left and inset). Optical microscopy of salt spray samples (right) indicates severity of substrate corrosion correlates with oxide thickness and degree of channel cracking.

Figure 8: Deposition of a uniform corrosion product suggests substrate composition is altered. FIB cross-sectioning (left) followed by EDS dot-mapping reveals a Cr-gradient between the bulk substrate and oxide layers. Overlayed Fe-Cr and O-Cr maps (middle) show development of layers, while individual element dot maps indicate relative amounts and areas of intensity for Fe, Cr, O used to create overlap maps.

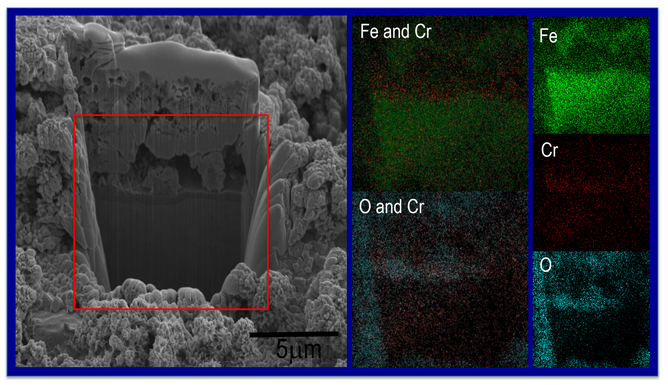

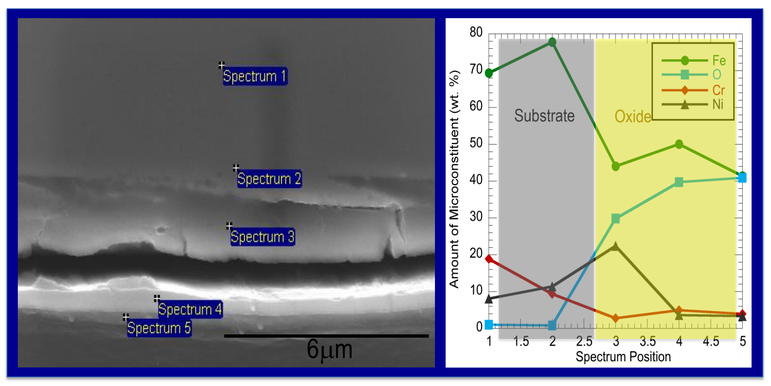

Figure 9: Metallographic cross sections examined with EDS spot profiles provide a semi-quantitative analysis of microconstituents. Cr content decreases near the substrate-oxide interface and then increases slightly in the oxide (positions shown on left, amounts in plot on right). Depletion of Cr from substrate increases susceptibility to salt water attack.

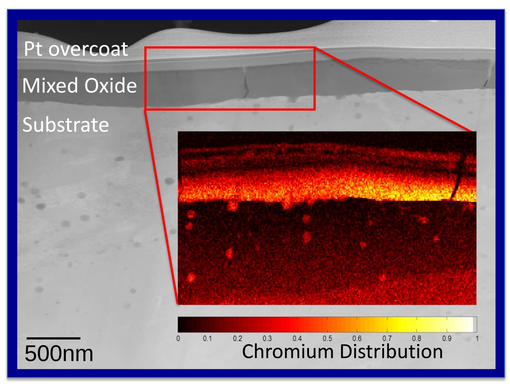

Figure 10: STEM EDS of an oxide-substrate interface which was not exposed to salt water also reveals a Cr gradient, further corroborating the proposal that substrate heating during laser processing results in Cr diffusion through the bulk substrate into the oxide leading to a Cr-depleted, "sensitized-like" microstructure immediately beneath the oxide that is prone to sea water attack.

Conclusions

- **Oxides grown via nanosecond pulsed laser irradiation are composed of multiple phases. The oxides have high residual stresses from formation which are relieved through cracking.**
- **Hardness and elastic modulus of oxides on CP Grade II Ti are relatively insensitive to processing parameters and undergo circumferential cracking at the plastic zone radius. Conversely, as oxides on SS 304L drop below 100nm in thickness, hardness decreases sharply and fracture shifts from circumferential to radial cracking. Surface channel cracking subsides for thickness less than ~150nm.**
- **Conducting nanoindentation manifests a unique correlation between laser processing parameters and oxide conductivity—faster laser scan rates correspond with higher conductivity, likely due to the presence of point defects such as vacancies as well as large defects such as through-thickness cracks.**
- **Immersion and salt spray testing results in corrosion of the steel immediately beneath the oxide indicating that surface cracks are through-thickness. Multiscale EDS reveals Cr depletion, increasing susceptibility to sea water and salt air attack. Thick oxides with pervasive surface cracking and very thin oxides which are not protective are particularly prone. Oxides with thicknesses on the order of 100nm are most immune to corrosion.**

Many thanks to David Saiz, Sergey Suslov, Jeff Chames, and Mark Rodriguez for sample fabrication, TEM, and XRD.

This work was partially supported by the Defense Threat Reduction Agency, Basic Research Award # IACRO 12-2026I, to Purdue University sub-contracted through Sandia National Laboratories.
Sandia National Laboratories is a multi-program laboratory managed and operated by Sandia Corporation, a wholly owned subsidiary of Lockheed Martin Corporation, for the U.S. Department of Energy's National Nuclear Security Administration under contract DE-AC04-94AL85000.

National Nuclear Security Administration

U.S. DEPARTMENT OF ENERGY